The Plant Journal (2007) **52**, 473–484 doi: 10.1111/j.1365-313X.2007.03249.x

The calcium sensor CBL10 mediates salt tolerance by regulating ion homeostasis in Arabidopsis

Beom-Gi Kim[1,†], Rainer Waadt[2,†], Yong Hwa Cheong[1,3,†], Girdhar K. Pandey[1], Jose R. Dominguez-Solis[1], Stefanie Schültke[2], Sung Chul Lee[1], Jörg Kudla[2,*] and Sheng Luan[1,*]

[1]*Department of Plant and Microbial Biology, University of California, Berkeley, CA 94720, USA,*

[2]*Institut für Botanik und Botanischer Garten, Universität Münster, Schlossplatz 4, 48149 Münster, Germany, and*

[3]*Department of Bio-Environmental Science, Sunchon National University, Suncheon, Jeonnam 540-742, Korea*

Received 7 April 2007; revised 14 June 2007; accepted 28 June 2007.

[*]For correspondence (fax +49 251 83 23311; e-mail jkudla@uni-muenster.de; fax +1 510 642-4995; e-mail sluan@nature.berkeley.edu).

[†]These authors contributed equally to this work.

Summary

Calcium serves as a critical messenger in many adaptation and developmental processes. Cellular calcium signals are detected and transmitted by sensor molecules such as calcium-binding proteins. In plants, the calcineurin B-like protein (CBL) family represents a unique group of calcium sensors and plays a key role in decoding calcium transients by specifically interacting with and regulating a family of protein kinases (CIPKs). We report here that the CBL protein CBL10 functions as a crucial regulator of salt tolerance in Arabidopsis. *Cbl10* mutant plants exhibited significant growth defects and showed hypersensitive cell death in leaf tissues under high-salt conditions. Interestingly, the Na^+ content of the *cbl10* mutant, unlike other salt-sensitive mutants identified thus far, was significantly lower than in the wild type under either normal or high-salt conditions, suggesting that CBL10 mediates a novel Ca^{2+}-signaling pathway for salt tolerance. Indeed, the CBL10 protein physically interacts with the salt-tolerance factor CIPK24 (SOS2), and the CBL10–CIPK24 (SOS2) complex is associated with the vacuolar compartments that are responsible for salt storage and detoxification in plant cells. These findings suggest that CBL10 and CIPK24 (SOS2) constitute a novel salt-tolerance pathway that regulates the sequestration/compartmentalization of Na^+ in plant cells. Because CIPK24 (SOS2) also interacts with CBL4 (SOS3) and regulates salt export across the plasma membrane, our study identifies CIPK24 (SOS2) as a multi-functional protein kinase that regulates different aspects of salt tolerance by interacting with distinct CBL calcium sensors.

Keywords: calcium sensor, salt stress, signal transduction, protein kinase, tonoplast.

Introduction

Soil salinity represents an increasingly prominent problem in agriculture. It is estimated that at least one third of the irrigated land in the world is now affected by salt. Because it is difficult physically to remove salt from the soil, improving crop tolerance to high salt becomes a critical task for breeders, and identifying molecular components conferring salt tolerance in plants can provide genetic markers for achieving this goal. Salt injury to plants is caused by ionic toxicity that is specific to a particular ion (such as Na^+), and osmotic stress that can also be induced by other conditions such as drought or low temperature (reviewed by Apse and Blumwald, 2002; Hasegawa *et al.*, 2000; Yeo *et al.*, 1998). The capability of plants to survive increased levels of salts is referred to as salt tolerance. Most important mechanisms for plant salt tolerance include osmotic adjustment and salt compartmentalization (Apse and Blumwald, 2002; Hasegawa *et al.*, 2000). Osmotic adjustment is achieved by the accumulation of compatible solutes in the cell to balance the osmotic gradient across the plasma membrane so that the cellular water status is maintained. The processes of salt compartmentalization generally include export of salt back to the exterior of the cell, translocation of salt to physiologically quiescent tissues (e.g. old leaves), and sequestration/storage in physiologically inert organelles (such as vacuoles). Common to these processes is that they enable plant cells to achieve a healthy balance (homeostasis) of

cytoplasmic ion levels (Blumwald, 2000; Niu *et al.*, 1993). Ion homeostasis involves movements of a large number of ions across cell membranes via the function of numerous transporters and channels with various ionic specificity and transport activity. Because NaCl is the most abundant salt encountered by plants under salinity stress conditions, transport systems that mediate the accumulation, exclusion, translocation and organelle sequestration of Na^+ and Cl^- are particularly important for plant salt tolerance (Flowers *et al.*, 2000; Munns *et al.*, 2006; Niu *et al.*, 1993). Transporters that mediate Na^+ uptake from the soil may include non-selective cation channels that have not so far been characterized at the molecular level (Amtmann *et al.*, 1999). Once Na^+ enters the cytosol, it can potentially be excluded (back to the soil) by Na^+/H^+ exchangers located in the plasma membrane, or sequestered into the vacuole by Na^+/H^+ exchangers (e.g. NHX proteins) located in the tonoplast (reviewed by Apse and Blumwald, 2002; Qiu *et al.*, 2003; Yokoi *et al.*, 2002). In addition, Na^+ must be translocated and redistributed to different parts of the plant through the vascular system. Salt redistribution plays a critical role in salt detoxification, as demonstrated by studies on two Na^+ transporters, AtHKT1 and SOS1, in Arabidopsis (Apse *et al.*, 1999, 2003; Berthomieu *et al.*, 2003; Qiu *et al.*, 2004; Rus *et al.*, 2004; Shi *et al.*, 2002). A critical role of HKT-type transporters in salt tolerance was also recently demonstrated in rice (Ren *et al.*, 2005).

Ca^{2+}-dependent pathways play critical roles in salt tolerance (reviewed by Luan *et al.*, 2002; Zhu, 2003). Earlier work implicated Ca^{2+} as second messenger in abiotic stress such as salinity responses (Knight, 2000; Sanders *et al.*, 2002). It is believed that Ca^{2+} transmits the stress signal further downstream in the pathway by binding to protein sensors. Particularly relevant is a family of calcium sensors named calcineurin B-like (CBL) proteins that function by interacting with a specific group of protein kinases designated as CIPKs (CBL-interacting protein kinases) (Luan *et al.*, 2002). Several CBLs and their target kinases have been shown to function in salt responses. CBL4 (SOS3) and its interacting kinase CIPK24 (SOS2) together with SOS1, an Na^+/H^+ exchanger at the plasma membrane, constitute a pathway that may function in Na^+ exclusion from the cytoplasm (Zhu, 2003). Other CBLs and CIPKs with established function in salt tolerance are CBL1 and its interacting kinase CIPK1, and CBL9 with its interacting kinase CIPK3 (Albrecht *et al.*, 2003; Cheong *et al.*, 2003; Pandey *et al.*, 2004; Shi *et al.*, 1999; G.K.P. and S.L., unpublished results). Common to all these CBL/CIPK signaling modules is that they contribute to salt tolerance by regulating processes at the plasma membrane. In contrast, little is known about the molecular nature of signaling components that mediate salt tolerance by regulating processes at internal cellular membranes. Here we describe the functional analysis of a novel CBL that, by interaction with a CIPK, regulates salt tolerance through such an alternative pathway.

Results

CBL10 is predominantly expressed in green tissues

Members of the CBL family of calcium sensors with an established function in regulating ion homeostasis exhibit a predominant expression in roots and contribute to ion uptake or exclusion from roots (Liu and Zhu, 1998; Xu *et al.*, 2006). To identify CBLs that may contribute to salt tolerance by an alternative mechanism, we analyzed the expression patterns of all CBLs based on the public gene chip databases. This preliminary search revealed that all *CBL* genes were significantly expressed in root tissues with the only exception of *CBL10*, which appeared to be predominantly expressed in aerial tissues of the plant. Moreover, the predicted CBL10 protein lacks N-terminal myristoylation and palmitoylation motifs, and instead harbors a unique N-terminal extension not shared by other CBLs, suggesting that CBL10 might have distinct functions (Batistic and Kudla, 2004). To confirm and extend the analysis of *CBL10* expression pattern, we examined *CBL10* mRNA levels in different plant organs using Northern blot and quantitative real-time polymerase chain reaction (RT-PCR) analysis. Both analyses indicated that the *CBL10* gene is expressed in green tissues, but no significant amounts of *CBL10* mRNA were observed in roots (Figure 1a,b). We also produced and analyzed transgenic plants harboring *CBL10* promoter–GUS fusion constructs and found that the GUS activity was associated with the cotyledons and leaves, but was not detected in roots (Figure 1c). In adult plants, in addition to leaves and stems, anthers also showed strong GUS activity. Further gene expression analyses indicated that *CBL10* was not induced by abiotic stress conditions such as high salt, drought or low temperature (data not shown).

Disruption of CBL10 *renders plants salt hypersensitive*

To approach the function of *CBL10*, we characterized a T-DNA insertional allele (SALK_056042) of the *CBL10* (At4 g33000) gene. The *CBL10* gene harbors nine exons and eight introns. The mutant contained a T-DNA insertion in the seventh intron after nucleotide 1264 from the start codon ATG (Figure 2a). PCR-based amplification and subsequent sequencing of T-DNA flanking regions revealed a deletion of 17 bp in the seventh intron, which would lead to a transcript encoding a truncated CBL10 protein without the fourth EF hand (Figure 2a). RT-PCR analysis showed that the insertion disrupted the expression of the *CBL10* gene (Figure 2b). For complementation, homozygous *cbl10* mutant plants were transformed with a genomic fragment containing the promoter, the coding region, and the 3′-UTR of the *CBL10* locus.

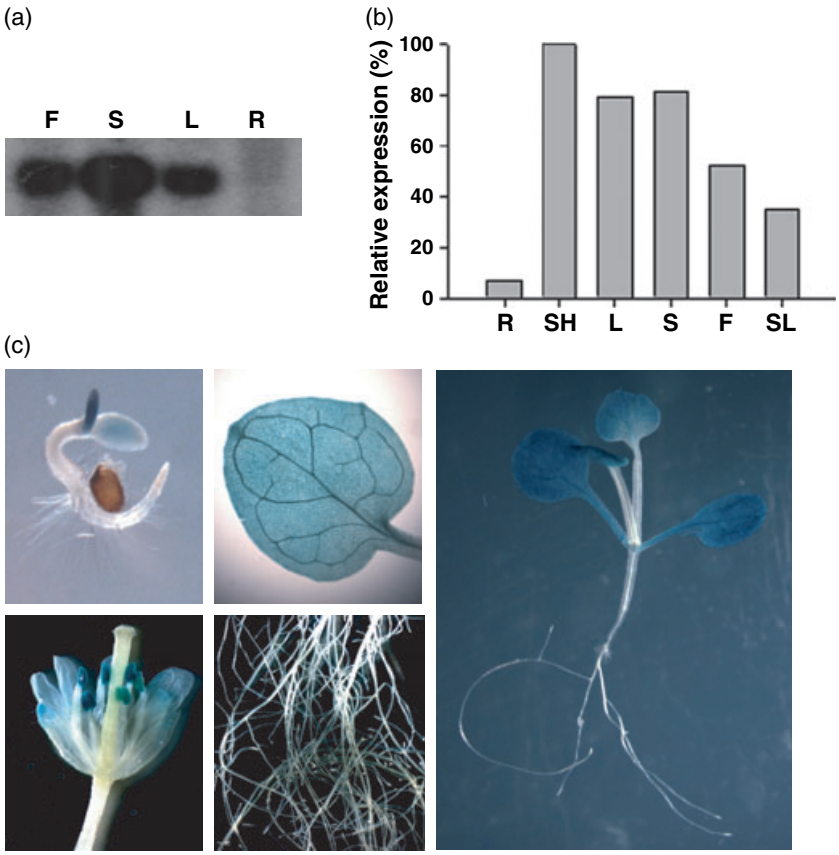

Figure 1. Expression pattern of the *CBL10* gene.
(a) Northern blot analysis of *CBL10* mRNA levels in flowers (F), stems (S), rosette leaves (L) and roots (R) of 4-week-old Arabidopsis plants grown under long-day conditions.
(b) Quantitative real-time polymerase chain reaction analysis of *CBL10* mRNA levels in roots (R), shoots (SH), rosette leaves (L), stems (S), flowers (F) and siliques (SL). The relative expression of the *CBL10* gene was calculated using *UBI10* as an internal reference.
(c) Histochemical (β-glucuronidase) GUS analysis of *CBL10* promoter-GUS transgenic plants. Clockwise from upper left: a 2-day-old seedling, a rosette leaf, a 2-week-old seedling, roots of a 3-week-old plant and a flower.

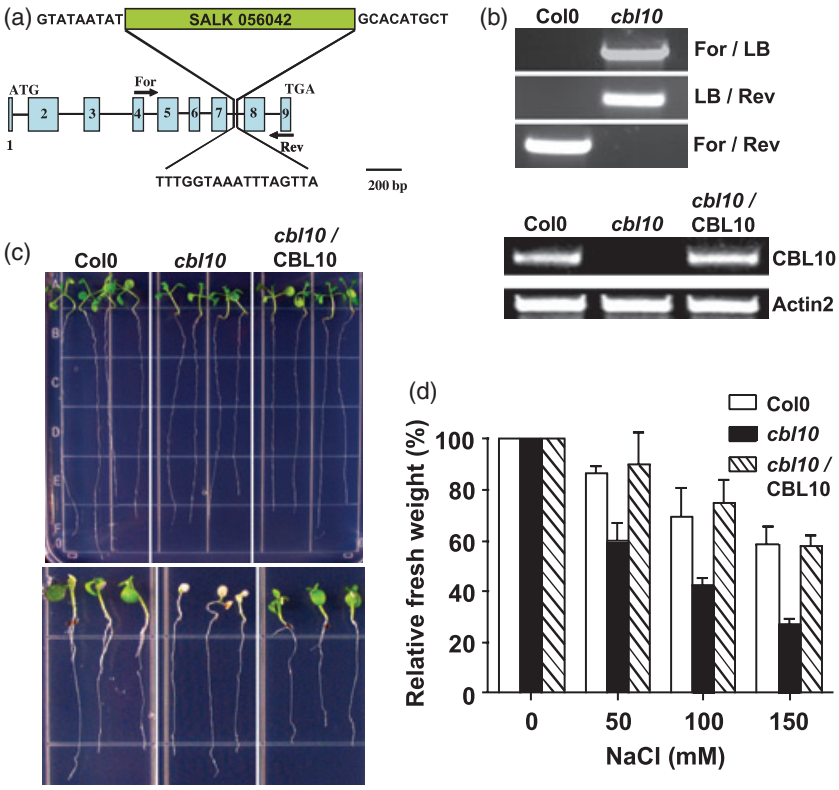

Figure 2. The *cbl10* mutant is hypersensitive to NaCl.
(a) Intron–exon structure of the *CBL10* gene and T-DNA location. Solid bars and lines indicate exons and introns, respectively. The position of the T-DNA insertion, sequences of the border flanking sites (upper side), the deleted 17 bp (lower side) and the primers (For and Rev) used for PCR are indicated.
(b) Polymerase chain reaction analysis of the T-DNA insertion in the homozygous *cbl10* mutant and wild-type plants with indicated primers (upper panel). PCR analysis of *CBL10* transcripts from the wild type, *cbl10* and a *cbl10*/CBL10 complementation line (lower panel). *Actin-2* expression level was analyzed as a quantification control.
(c) Post-germination assay of *cbl10* seedlings. Four-day-old seedlings were transferred to 0.5 MS medium with (lower panel) or without (upper panel) 175 mM NaCl. Photographs were taken 6 days after the transfer.
(d) Relative FW of seedlings grown on NaCl media. Four-day-old seedlings were transferred to 0.5 MS media containing various concentrations of NaCl. FW was measured 6 days after transfer. Average values ± SE of three independent experiments.

The expression of the *CBL10* gene was restored in complementation lines (Figure 2b).

We examined *cbl10* mutant plants under normal growth conditions in the glasshouse and did not observe significant differences from the wild type. In germination and post-germination assays under various abiotic stress conditions (Pandey *et al.*, 2004), we found that the *cbl10* mutant is specifically hypersensitive to salt stress. We performed initial salt stress assays with wild type, *cbl10* mutant and three independent complementation lines (numbered 4–6). After we confirmed that the wild type and the three complemented lines showed a similar phenotype in these analyses, we conducted detailed analyses using the wild type, *cbl10* mutant and one complementation line (number 4). These analyses indicated that *cbl10* mutant seedlings were more sensitive to high-salt medium following germination and transfer from the normal medium (Figure 2c,d). The cotyledons of *cbl10* mutant plants were bleached 5 days after transfer to medium containing 175 mM NaCl (Figure 2c), whereas wild-type and complemented lines were not as severely affected. We performed post-germination assays using several different NaCl concentrations and scored FW of seedlings as a growth indicator. As shown in Figure 2d, growth of the mutant was consistently more inhibited than the wild type when grown in medium containing 50 mM or more NaCl. However, consistent with the results depicted in Figure 2, the root growth in mutant and wild-type plants was not differently affected. Because the complemented lines showed similar salt tolerance to the wild type, NaCl hypersensitivity of the *cbl10* mutant is caused by disruption of the *CBL10* gene.

We also compared the wild-type and *cbl10* plants with *cbl4* and *sos2-2* mutant lines in a salt-tolerance assay (Figure S1a in Supplementary Material). On the medium containing 100 mM NaCl, root growth of *cbl4* and *sos2-2* plants, but not *cbl10* mutant, was significantly inhibited as compared with the wild type. However, under these stress conditions the FW of both *sos2-2* and *cbl10* mutant plants was more severely reduced compared with the *cbl4* mutant (Figure S1a).

To extend the salt-tolerance assays to adult plants, we treated 5-week-old plants that just started to bolt with 300 mM NaCl (Cheong *et al.*, 2003). Under control conditions (treated with water), the growth of *cbl10* mutant plants was similar to the wild type or the complemented line. However, the elongation of the stems in *cbl10* mutant plants was more severely inhibited upon NaCl treatment, and the stem collapsed 7 days after NaCl treatment. The collapsed stems were wilted and dry, and died within 10 days after Na^+ treatment, whereas wild-type plants retained their stature (Figure 3a). Stem length of mutant plants was less than 50% of wild type before the collapse (Figure 3b). Rosette leaves of *cbl10* mutant plants contained less chlorophyll (Chl) than the wild type 7 days after NaCl treatment (Figure 3d), and turned yellow 10 days after NaCl treatment (Figure 3c). Taken together, these data indicate that loss of *CBL10* function impairs Na^+

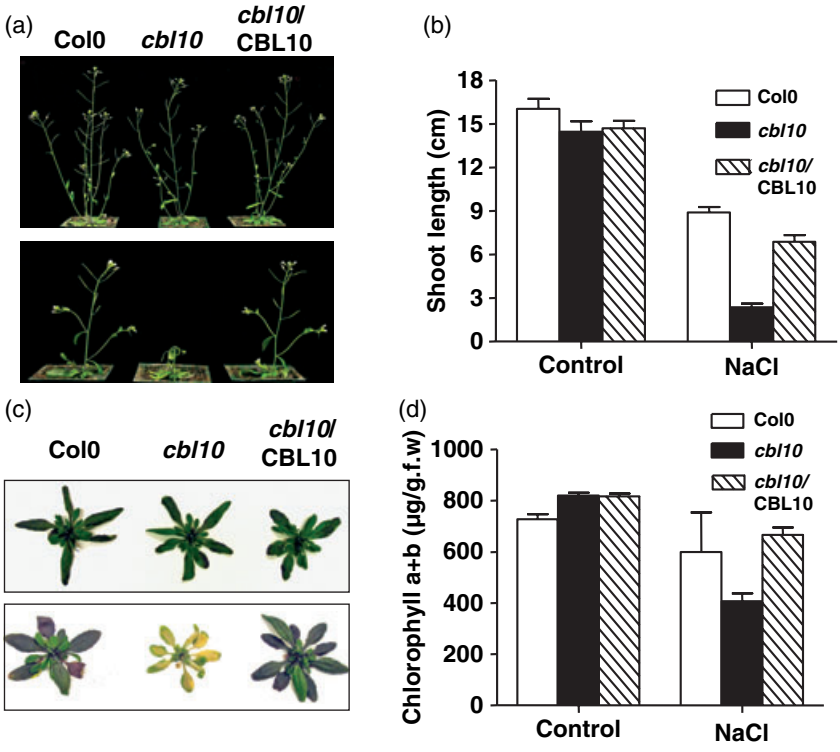

Figure 3. Mature *cbl10* mutant plants are hypersensitive to NaCl.
(a) Shoot growth of mature *cbl10* mutant plants is inhibited by NaCl. Upper panel, plants treated with water. Lower panel, plants treated with 300 mM NaCl.
(b) Shoot length of plants after NaCl treatment.
(c) Rosette leaves of mature plants treated with water (upper panel) or 300 mM NaCl (lower panel).
(d) Chorophyll content of plants treated with NaCl. Results depicted in (b) and (d) are average values ± SE of three independent experiments. Photographs were taken from 5-week-old plants, 10 days after treatment.

tolerance at various developmental stages. It is important to note that, unlike the previously reported salt-sensitive mutants, the *cbl10* mutant displays salt-sensitive phenotypes specifically in leaves or shoots, but not in root growth, consistent with the green tissue-specific expression of the *CBL10* gene.

Salt hypersensitivity of the cbl10 *mutant results from ionic toxicity*

To determine whether salt sensitivity of the *cbl10* mutant was caused by ionic or osmotic stress, we tested the *cbl10* mutant on medium containing a different salt, LiCl, as Li^+ is a more toxic ionic analog for Na^+ (Wu *et al.*, 1996). We also analyzed mutant plants on medium containing mannitol, which mimics osmotic stress without exerting ionic toxicity. The *cbl10* plants displayed hypersensitivity to both NaCl and LiCl, but not to mannitol (Figure 4a). These results indicate that the reduced salt tolerance in the *cbl10* mutant is caused by enhanced ionic toxicity.

The cbl10 *mutant retains a lower sodium content*

To examine what underlies the more severe ionic toxicity in the *cbl10* mutant, we determined the sodium and potassium content of wild-type, *cbl10* mutant and complemented plants grown in MS medium on Petri dishes or in liquid culture (Figure 4b,c). Surprisingly, *cbl10* mutant plants, in contrast to all salt-sensitive mutants investigated so far (Rus *et al.*, 2004; Zhu, 2003), consistently contained less Na^+ than the wild type and complemented plants under either normal or high-salt conditions. Furthermore, and in contrast to the observations with other mutants, the K^+ content in the *cbl10* mutant was higher than in the wild type (Figure 4b,c) under NaCl stress. To extend our analyses to adult plants cultivated under more natural conditions, we also determined the Na^+ and K^+ content of plants grown for 3 weeks in soil. These analyses again revealed a reduced Na^+ content and an increased K^+ concentration in the *cbl10* mutant plants (Figure 4d). A lower K^+/Na^+ ratio is a typical characteristic of previously identified salt-sensitive mutants. However, our analyses have identified a salt-sensitive mutant with a significantly higher K^+/Na^+ ratio than the wild-type plants, suggesting that CBL10 regulates a novel pathway that functions in ion homeostasis (Ren *et al.*, 2005; Rus *et al.*, 2004).

CBL10 physically interacts with and recruits CIPK24 to the vacuolar membrane

Physical and functional interaction between CBL-type calcium sensors and CIPK family kinases constitutes a major paradigm in Ca^{2+} signal transduction in plants. We used the yeast two-hybrid system to test interaction between CBL10 (in the AD vector) and each of the 25 CIPKs (in the BD vector), and identified CIPK24 as a strong interactor of CBL10 (Figure 5a). To confirm the interaction between CBL10 and CIPK24, His-tagged CBL10 and CIPK24 fused to GST (glutathione *S*-transferase) were expressed in *Escherichia coli* and

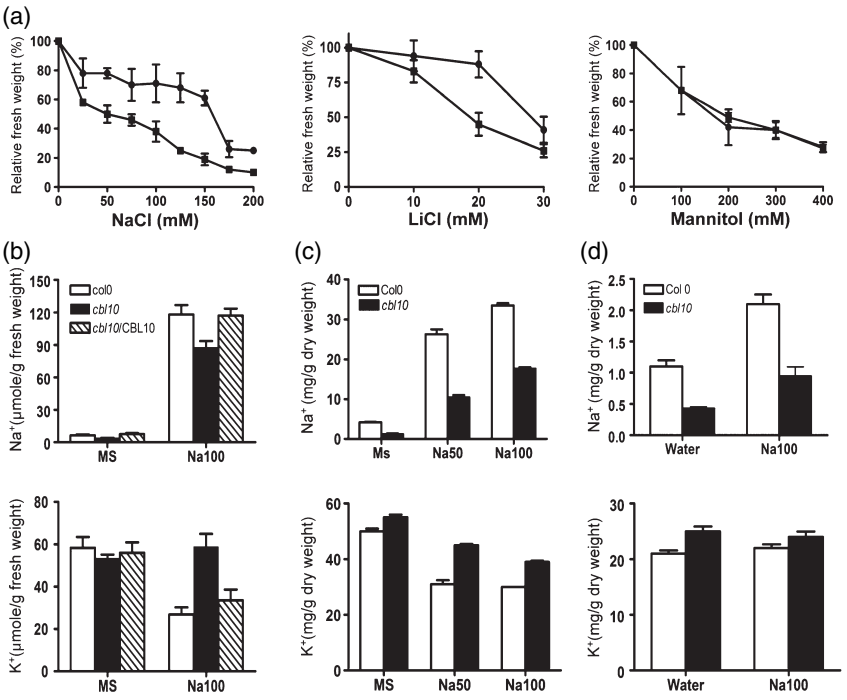

Figure 4. NaCl hypersensitivity of the *cbl10* mutant is caused by defects in ion homeostasis.
(a) *cbl10* is hypersensitive to Na^+ and Li^+ but not to mannitol.
FW of *cbl10* mutant (squares) and wild-type (circles) plants grown in 0.5 MS media supplemented with different concentrations of NaCl (left), LiCl (middle), or mannitol (right) was measured and compared with the 0.5 MS control.
(b) Na^+ and K^+ content in seedlings grown on vertical 0.5 MS agar plates.
(c) Na^+ and K^+ content in seedlings grown in liquid culture.
(d) Na^+ and K^+ content in soil-grown plants.
Results in (a–d) depict average values ± SE of three experiments.

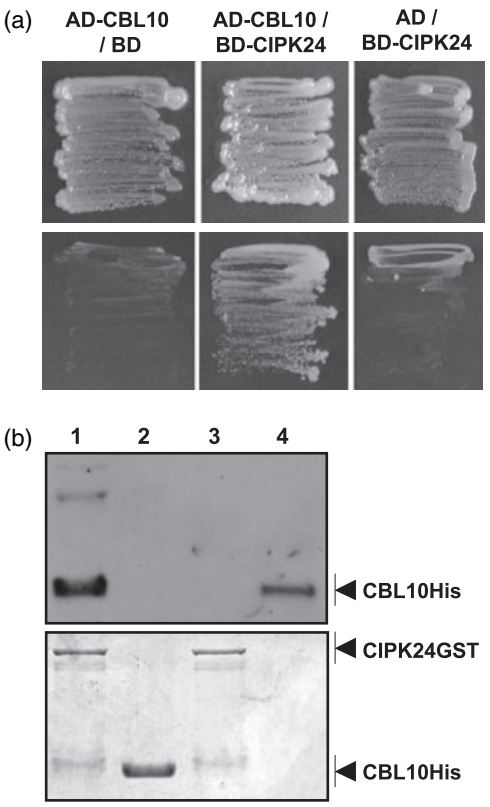

Figure 5. CBL10 interacts with CIPK24.
(a) Interaction of CBL10 and CIPK24 as shown by yeast two-hybrid assays. Yeast was grown on SC-L-T medium (upper row; see Experimental procedures) or on SC-L-T-H medium containing 1.5 mM 3-AT (lower row).
(b) Interaction of CBL10 and CIPK24 in a pull-down assay. Upper panel, Western blot probed with a His antibody; lower panel, Coomassie blue-stained gel. Lanes 1 and 2 contained pull-down products of CBL10-His mixed with GST–CIPK24 (lane 1) or GST (lane 2) immobilized to glutathione beads. Lanes 3 and 4 were loaded with CIPK24–GST bead only (lane 3) or with purified CBL10-His (lane 4).

purified. CIPK24–GST protein was immobilized to glutathione beads and His-tagged CBL10 protein was incubated with the beads in a pull-down assay. In this analysis, the CBL10 protein co-purified with CIPK24–GST but not with GST, indicating a specific interaction between CBL10 and CIPK24 (Figure 5b).

To assess the subcellular localization of CBL10 and CIPK24 in plant cells, we analyzed the localization of GFP fusions in leaf epidermal cells and in protoplasts from transiently transformed *Nicotiana benthamiana* leaves (Figure 6). We included as controls the plasma membrane-localized calcium sensor CBL1, as well as GFP, which is known to localize to the cytoplasmic and nuclear compartments (D'Angelo *et al.*, 2006). Both GFP and GFP::CIPK24 exhibited typical cytosolic and nuclear fluorescence (Figure 6). In contrast, the fluorescence of the CBL10::GFP fusion protein was localized to membraneous compartments, which surrounded the nucleus as membrane invaginations (yellow arrows in Figure 6) as well as to fast-moving punctate structures in the cytoplasmic compartment of the cell (white arrows in Figure 6). In addition, we analyzed the localization of a GFP fusion construct in which CBL10 was fused to the C-terminus of GFP. The GFP::CBL10 fusion protein was also observed mainly to be associated with highly mobile punctate structures indicative for localization in the endosomal compartments (Figure 6) and to membraneous invaginations that are likely to represent vacuolar membranes (the tonoplast). The localization of both CBL10 GFP fusion proteins was clearly distinct from the nuclear, cytoplasmic or plasma membrane localization of the other GFP fusion proteins that were also examined for comparison. To further determine the identity of these internal membranes, we purified vacuoles from *N. benthamiana* leaves expressing GFP::CBL10 fusion proteins. Microscopic analyses of these organelles unambiguously identified CBL10 as a tonoplast-associated protein (Figure 6).

In addition, we generated stably transformed Arabidopsis lines that constitutively expressed GFP::CBL10 fusion protein in the *cbl10* mutant background. Importantly, expression of GFP::CBL10 complemented the salt-sensitive phenotype of the mutant line, thereby establishing the proper functionality of the expressed fusion proteins (Figure S1b). As observed in transiently transformed *N. benthamiana* cells, GFP fluorescence in these plants was detected at the tonoplast (Figure S1c).

To further address the identity of the fast-moving punctate structures, we performed co-localization analyses with mRFP (monomeric red fluorescent protein) fusions of the marker proteins ARA6 and ARA7, which have been shown to localize to distinct populations of endosomes (Ueda *et al.*, 2004). In particular, it has been suggested that the ARA7 locations represent the pre-vacuolar compartments (PVC) (Lee *et al.*, 2004). The GFP::CBL10 fusion protein exhibited a localization overlapping with, but not identical to, ARA6 (Figure 7A:a–c) or ARA7 (Figure 7A:d–f), suggesting that this calcium sensor localizes to a population of endosomes that may include the PVC.

We also performed comparative localization analyses of CBL10::GFP and CBL1::GFP with the fluorescent marker dye FM4-64 to clarify the identity of membranes at which CBL10 localization was observed. FM4-64 has been characterized as an endocytotic marker dye that is internalized from the plasma membrane to the tonoplast via the endosomal compartment (Dettmer *et al.*, 2006; Ueda *et al.*, 2001). Application of FM4-64 to *N. benthamiana* leaf discs results in a red labeling of the plasma membrane (Figure 7B:h,k). Expression of the plasma membrane-localized CBL1::GFP in the same cells (Figure 7B:j) gave rise to an identical staining pattern as observed in the overlay of both localization analyses (Figure 7B:l). In contrast, the localization of CBL10::GFP was clearly different from the

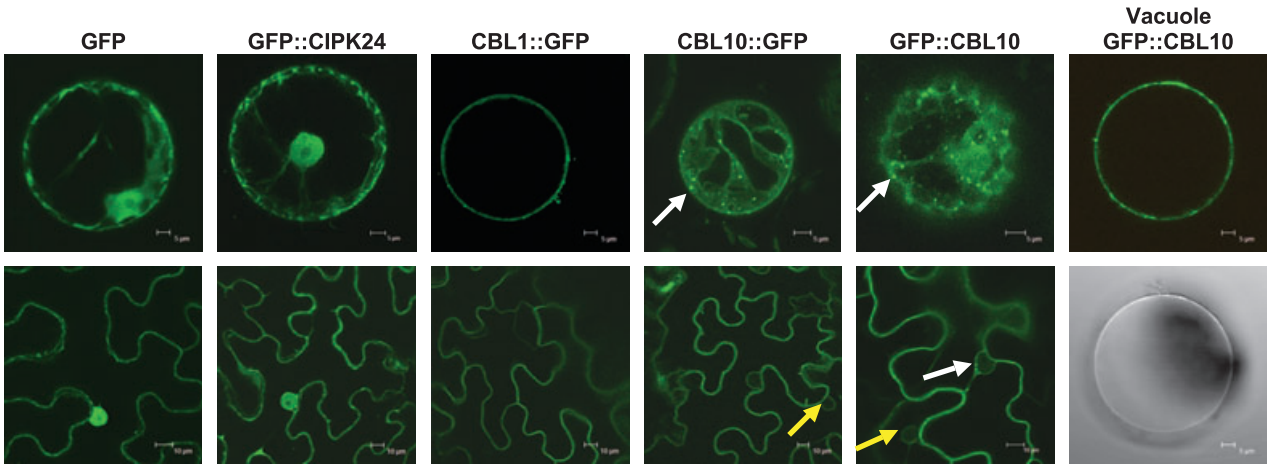

Figure 6. CBL10 is localized to punctate structures and vacuolar membranes.
Upper row, protoplasts (bars = 5 μm) generated from *Agrobacterium*-infiltrated *Nicotiana benthamiana* leaves; lower row, leaf epidermis cells (bars = 10 μm). Images on the right show GFP::CBL10 fluorescence from an isolated vacuole (upper side) and the bright-field image (lower side, bars = 5 μm). White arrows, punctate structures; yellow arrows, vacuolar membraneous invagination surrounding the nucleus.

localization of FM4-64 (Figure 7B:g,h,i) and was observed at the vacuolar membranes forming the nuclear pocket and invaginations into the intracellular space. In addition, we tested co-localization with the vacuolar membrane marker protein TPC1 (Peiter *et al.*, 2005) for additional corroboration of the tonoplast localization of CBL10. To this end a TPC1::OFP fusion protein was co-expressed in *N. benthamiana* cells with either CBL1::GFP or GFP::CBL10 (Figure 7C). The overlay analyses of green GFP::CBL10 fluorescence with the red TPC1::OFP emission pattern clearly indicated a co-localization of the two proteins (Figure 7C:o). In contrast, the fluorescence patterns of CBL1::GFP and TPC1::OFP were distinct and did not display yellow fluorescence in the overlay analysis (Figure 7C:r).

To further corroborate the observed localization pattern and to investigate the CBL10–CIPK24 interaction *in vivo*, we performed co-localization studies and bimolecular fluorescence complementation (BiFC) analyses in transiently transformed *N. benthamina* leaves (Walter *et al.*, 2004). In this system, an enhanced YFP is split into N- and C-terminal fragments that are fused with two potentially interacting proteins. Interaction of the two proteins of interest results in re-assembly of a functional YFP and restoration of fluorescence emission, which is not observed in the absence of protein interaction (Hu and Kerppola, 2003; Walter *et al.*, 2004). Because mutation of CBL1 also renders plants salt-sensitive (Albrecht *et al.*, 2003), and because CBL1 has been shown to interact with CIPK24 (Kolukisaoglu *et al.*, 2004), we included this calcium sensor protein in our interaction studies. The fluorescence pattern in the BiFC protein–protein interaction analyses of CBL10 and CIPK24 revealed a localization of CBL10–CIPK24 complex formation at an intracellular membrane (Figure 8a,c) that is clearly distinct from the pattern of the plasma membrane localization displayed by the CBL1–CIPK24 complex (Figure 8j,l). As expected, CIPK24 lacking the CBL-interacting domain (CIPK24NAFΔ) did not interact with CBL10 or CBL1, and failed to produce significant fluorescence. As observed previously in BiFC studies in *N. benthamiana* leaves (Walter *et al.*, 2004), some non-specific weak background fluorescence could be observed in these cells, which allowed the detection of transformed cells (Figure 8b,k) and further supported that the strong BiFC fluorescence was specifically produced by CBL10–CIPK24 (Figure 8a,c) and CBL1–CIPK24 (Figure 8j,l) interaction. In more detailed analyses, we performed co-staining with dihydrochloride monohydrate (DAPI) and FM4-64 that label the nucleus and plasma membrane, respectively. Accordingly, we observed co-localization of FM4-64 and the CBL1–CIPK24 complex (Figure 8m–o). In contrast, the fluorescence produced by the CBL10–CIPK24 complex was distinct from the FM4-64-labeled plasma membrane and appeared around the large central vacuole (Figure 8d–f). In addition, the nucleus appeared between CBL10–CIPK24 fluorescence and FM4-64-stained plasma membrane (Figure 8f), clearly distinct from the pattern shown in the CBL1–CIPK24 cell (Figure 8o). This pattern of localization was consistently observed in cells expressing CBL10 and CIPK24. In an additional series of experiments, we co-expressed the vacuolar marker protein TPC1 as orange fluorescent protein (OFP) fusion with the BiFC plasmid combinations for either CBL1–CIPK24 or CBL10–CIPK24 in *N. benthamiana* cells. These analyses revealed co-localization of TPC1::OFP (red fluorescence in Figure 8h) and the fluorescence generated by the CBL10–CIPK24

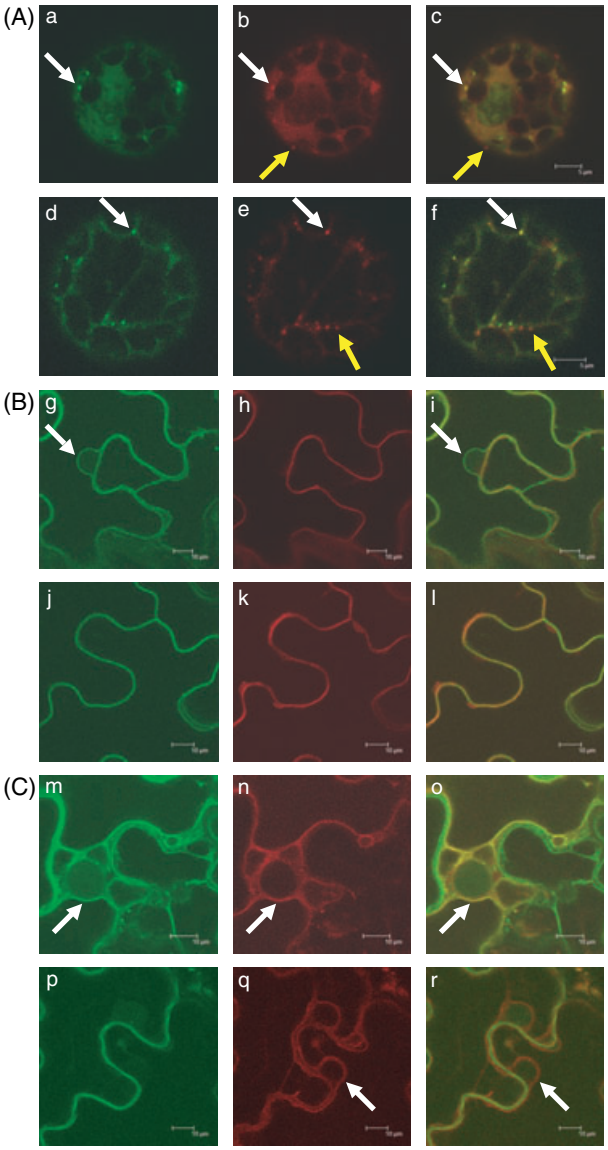

Figure 7. CBL10 co-localizes with endosomal and tonoplast marker proteins.
(A) Co-localization analyses of GFP::CBL10 (green) with mRFP-tagged endosomal markers ARA6 (a–c) and ARA7 (d–f, red). Merged images of green and red channels are presented in (c,f). White arrows point to co-localization; yellow arrows indicate non-overlapping localization (bars = 5 μm).
(B) Co-localization analyses of CBL10::GFP (g–i) and CBL1::GFP (j–l, green) with the fluorescent marker dye FM4-64 (red) labeling the plasma membrane. Merged images are shown in (i,l). White arrows, membraneous invaginations surrounding a nucleus distinct from FM4-64 (bars = 10 μm).
(C) Co-localization analyses of GFP::CBL10 (m–o) and CBL1::GFP (p–r, green) with the tonoplast marker TPC1::OFP (red). Merged images are shown in (o,r). White arrows, vacuolar membrane forming nuclear pockets; yellow in (o) shows co-localization of GFP::CBL10 and TPC1::OFP (bars = 10 μm).

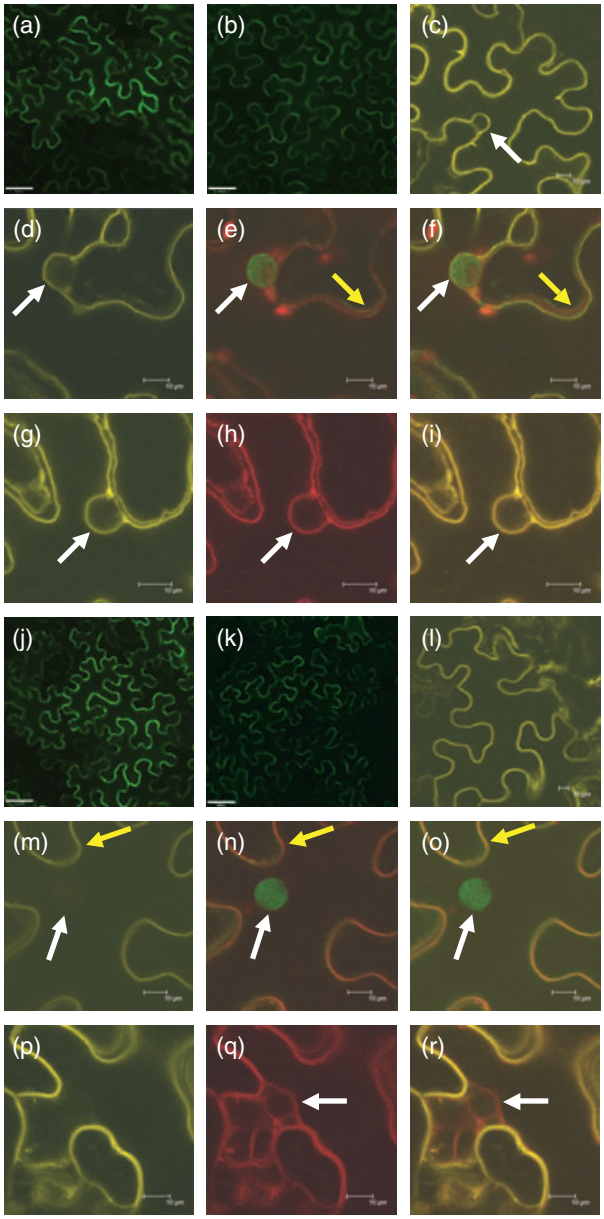

Figure 8. CBL10 interacts with CIPK24 at the tonoplast.
Bimolecular fluorescence complementation and co-localization analyses of CBL10::YC/YN::CIPK24 (a,c–i); CBL10::YC/YN::CIPK24NAFΔ (b), CBL1::YC/YN::CIPK24 (j,l–r); CBL1::YC/YN::CIPK24NAFΔ (k, yellow), with FM4-64/DAPI and TPC1::OFP. (a,b,j,k) Images were taken with an inverted fluorescence microscope (bars = 50 μm). All other images were taken using confocal laser scanning microscopy. FM4-64-stained plasma membrane (red), auto-fluorescent chloroplasts (red), and DAPI-stained nuclei (green) are shown in (e,n). Merged images of (d and e), (m and n) are depicted in (f,o), respectively. The tonoplast marker TPC1::OFP (red) is shown in (h,q). Images in (i,r) are produced by merging (g and h), (p and q), respectively. White arrows, position of nucleus; yellow arrows, FM4-64-stained plasma membrane (bars = 10 μm).

complex (yellow fluorescence in Figure 8g) as shown in the overlay image (Figure 8i). In contrast, the localization of plasma membrane-tethered CBL1–CIPK24 complex was clearly distinct from the localization observed for TPC1::OFP (Figure 8p–r).

Taken together, these data establish that the CBL10–CIPK24 complex is localized at the tonoplast, supporting the hypothesis that interaction of CBL10 with CIPK24 recruits the complex to the vacuolar membrane, where CIPK24 may

regulate transport proteins involved in vacuolar sequestration of Na^+.

Discussion

When plants encounter high-salt conditions, Ca^{2+} concentration in the cytoplasm increases, initiating Ca^{2+} signaling mechanisms required for salt detoxification and ionic homeostasis (Luan *et al.*, 2002; White *et al.*, 2002). At the cellular level, salt detoxification can occur through two distinct pathways. One is to export the toxic ions across the plasma membrane to the exterior of the cell, and the other is to store/sequester the ions into organelles especially the vacuole (Hasegawa *et al.*, 2000). In this report we have identified Ca^{2+}-signaling components that appear to regulate salt detoxification through vacuolar sequestration. These signaling components include the CBL calcium sensor CBL10 and its target kinase CIPK24, which form a CBL–CIPK complex at the vacuolar membrane and are required for salt tolerance in Arabidopsis, as shown by genetic analysis.

Earlier studies have shown that a Ca^{2+} signal-transduction pathway is also involved in the regulation of sodium export to the cell exterior. That pathway consists of the plasma membrane-localized CBL4 (SOS3) calcium sensor, the interacting kinase CIPK24 (SOS2), and a plasma membrane Na^+/H^+ antiporter SOS1 (Qiu *et al.*, 2003; Shi *et al.*, 2002). Because the *sos1* mutant is hypersensitive to salt and contains more salt than the wild type, it is believed that the SOS1 protein may exclude Na^+ from the cytoplasm and eventually from plants. Although disruption of CIPK24 (SOS2) and CBL4 (SOS3) also causes a salt-hypersensitive phenotype, these mutant plants, unlike the *sos1* mutant, do not contain significantly more Na^+ than the wild type, indicating that CIPK24 (SOS2) and CBL4 (SOS3) may have additional functions other than regulating SOS1. Interestingly, the newly identified *cbl10* mutant contained significantly less Na^+ than the wild type, despite its salt-hypersensitive phenotype. A lower Na^+ content in a salt-sensitive mutant has not been reported previously, indicating that CBL10 may regulate a novel pathway for salt tolerance. Reduced salt accumulation in plants can result from less uptake into, or more export from, the plants. However, plants with less uptake or more export of salt should be more resistant to salt stress. Another possible pathway leading to lower Na^+ content in the cell is a lower capacity for sequestering salt into the vacuole, which sequesters 90% of toxic salts in a cell. A defective pathway for vacuolar Na^+ sequestration would result in salt sensitivity because Na^+ from the cytoplasm can not be effectively stored away into the vacuole. Because of less vacuole storage, less salt would get into plant cells before the cells die from salt toxicity. This scenario would explain why the *cbl10* mutant plants contained less Na^+ than the wild type, although they are more sensitive to salt. Also consistent with this hypothesis is the finding that overexpression of AtNHX1 (a vacuolar Na^+/H^+ antiporter) renders plants salt-tolerant, although the Na^+ content of these plants is higher than the control (Apse *et al.*, 1999). The high Na^+ content in these plants may result from more efficient Na^+ sequestering into the vacuole reducing salt content in the cytoplasm, where Na^+ causes cell toxicity (Apse *et al.*, 1999). Further support for a function of CBL10 in vacuolar sequestering processes comes from the results that CBL10 interacts with CIPK24, and that this CBL–CIPK complex is associated with the tonoplast. Interestingly, we noted that, in addition, CBL10 alone appears to be located in endosomal compartments, which may represent the PVC. Similarly, CIPK24 alone was also localized to other parts of the cell instead of the vacuole. We speculate that CBL10 and CIPK24 may each interact with more than one partner, and interaction with a specific partner may determine the location of the CBL–CIPK complex. This idea is supported by the finding that CBL10 and CBL4 both interact with CIPK24, but the location of the complexes is different. When interacting with CBL4, CIPK24 was reported to regulate plasma membrane Na^+/H^+ antiporter activity (Zhu, 2003). Here we show that by interacting with another partner CBL10, CIPK24 may regulate vacuolar transporters for Na^+ sequestration. Such transporters could include Na^+/H^+ antiporters as suggested earlier by studies detecting a lower vacuolar Na^+/H^+ antiporter activity in *sos2* (*cipk24*) mutant plants (Qiu *et al.*, 2004). In addition to the finding that localization of CIPK24 depends on the CBL member it interacts with, the expression pattern of CBLs and CIPKs may also play a role in determining the specific function of the CBL–CIPK complexes. While CIPK24 is expressed throughout the plant, CBL4 and CBL10 each have a tissue-specific expression pattern. The CBL4 gene is mainly expressed in the roots, whereas CBL10 is expressed almost exclusively in the green tissues. Consistent with these expression patterns, *cbl4* mutants exhibited a reduced root growth under salt stress, a phenotypic change that was not significantly affected in the *cbl10* mutant (Figure S1a). Remarkably, the *sos2-2* mutant appeared to share the reduced root-growth phenotype with *cbl4*, and cotyledon-bleaching phenotypes with *cbl10* (Figure S1a). Therefore CIPK24 in roots may predominantly interact with CBL4 to regulate plasma membrane Na^+/H^+ antiporters leading to Na^+ exclusion. In shoots, the CBL10–CIPK24 complex may be the major complex that plays a role in Na^+ sequestration into the vacuole (Figure 9). The alternative mechanisms in the roots and shoots also coincide with the environments of the organs, namely that roots can export salts directly back to the soil, whereas the immediate strategy available for shoots is to sequester Na^+ into the vacuole.

Ion homeostasis is important not only in salt tolerance, but also in plant nutrition. In addition to the findings that CBL4–CIPK24 and CBL10–CIPK24 function in salt response-

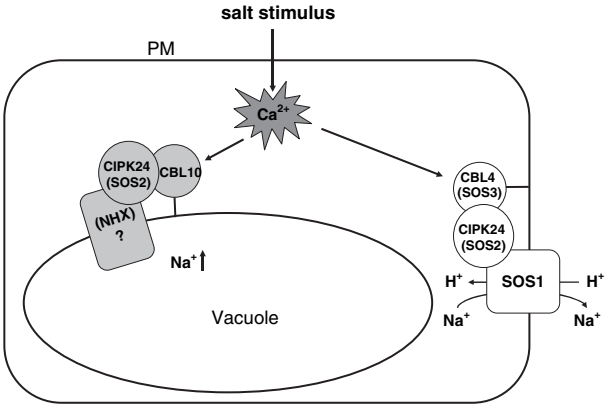

Figure 9. Hypothetical model of CBL10 function.
Na^+ stress triggers cytosolic Ca^{2+} elevation that targets CBL4 (SOS3) and CBL10. Both calcium sensors can interact with CIPK24 (SOS2), forming alternative calcium sensor–kinase complexes. The CBL4–(SOS3)–CIPK24 (SOS2) complex targets the plasma membrane localized Na^+/H^+ exchanger SOS1; the CBL10–CIPK24 (SOS2) complex regulates ion-transport processes at the vacuolar membrane.

signaling pathways, several other CBLs and CIPKs have been reported to play a role in general stress responses and K^+ nutrition in Arabidopsis. In particular, a signaling pathway for low-K^+ response involves two CBLs (CBL1 and CBL9) and their common target CIPK23. Instead of having different functions, as in the case of CBL4 and CBL10, the calcium sensors CBL1 and CBL9 function synergistically in regulating CIPK23 which, in turn, targets and activates the potassium channel AKT1 and leads to enhanced uptake of K^+ from the soil/medium (Li *et al.*, 2006; Xu *et al.*, 2006). As both salt tolerance and K^+ nutrition are mediated by a number of transporters, we postulate that the CBL–CIPK signaling network serves a major function in regulating the activity of these transporters, thereby controlling plant salt tolerance and mineral nutrition (Hedrich and Kudla, 2006; Pardo *et al.*, 2006).

Experimental procedures

Plant materials and gene expression analysis

Arabidopsis thaliana ecotype Columbia 0 (Col 0) was used in all experiments and cultivated either in MS medium or in soil, as described earlier (Cheong *et al.*, 2003; Pandey *et al.*, 2004). The *sos2-2* mutant allele used in this study was kindly provided by Dr Yan Guo. The *cbl4* mutant allele was isolated from the GABI collection (GABI_015F02). The *cbl10* mutant allele (SALK 056042) was isolated from the T-DNA-transformed Arabidopsis collection from the Arabidopsis Biological Resource Center (http://www.biosci.ohio-state.edu/pcmb). The T-DNA insertion position in the gene was confirmed by PCR using T-DNA border primers and *CBL10* gene-specific primers followed by DNA sequencing of the PCR products for both flanking sides. Co-segregation analyses of the T-DNA insertion with the kanamycin marker gene of the T-DNA in a segregating F_2 population revealed a single T-DNA insertion in this transgenic line. For complementation, a 3.9-kb genomic DNA fragment of the *CBL10* gene including 1.97 kb of the 5′-flanking region upstream from the ATG start codon, the complete coding region, and the 3′-UTR was used to transform *cbl10* mutant plants by the floral dip method (Clough and Bent, 1998). Seedlings were selected on plates containing 15 μg ml^{-1} hygromycin and transplanted to soil. Homozygous complemented lines (denoted *cbl10*/CBL10) were used for further analysis.

Total RNA (10 μg) was isolated using a Tripure isolation reagent (Roche Diagnostics, http://www.roche.com/home.html) and *CBL10* mRNA levels in different tissues were measured by Northern blot and quantitative RT-PCR analysis as described previously (Cheong *et al.*, 2003; D'Angelo *et al.*, 2006). For *CBL10* promoter–GUS reporter analysis, a putative 1.97-kb *CBL10* gene promoter was amplified by PCR and cloned into the PBI101 vector to transform wild-type Arabidopsis (Col-0) plants. T_2 seedlings from five different individual lines were analyzed for expression patterns, as described earlier (Pandey *et al.*, 2004). Homozygous *cbl10* mutant plants were stably transformed with GFP::CBL10 driven by the MAS-promoter in the binary vector pGPTVIIbar-pMASGFP::CBL10 (Walter *et al.*, 2004). Homozygous T_3 plants were used for phenotypic analyses.

Ion-stress treatment and phenotypic analyses

For stress treatments and FW measurements, 4-day-old seedlings from vertical MS plates were transferred onto MS plates supplemented with salts or mannitol. Plants of different genotypes (wild type, *cbl10* or *cbl10*/*CBL10*) were placed on the same plate, and three replicate plates were used for each treatment. Ten seedlings from each genotype were collected on each plate, and their total FW was measured. The percentage value of salt- or mannitol-treated plants versus plants grown under normal conditions was used to present the data. For salt-tolerance assays, 4-week-old, long-day-grown plants starting to bolt were treated with 300 mM NaCl once every 3 days for 2 weeks. Photographs were taken 10 days after the first treatment. Chlorophyll was extracted using dimethyl sulphoxide as described earlier (Barnes *et al.*, 1992). Arnon's equations were used to calculate the Chl contents (Arnon, 1949).

Measurement of Na^+ and K^+ content

Five-day-old seedlings were transferred to vertical plates containing 0.5 MS agar medium with or without 100 mM NaCl. Seven days after transfer, plant shoots were harvested, ground and resuspended in 2 ml water. The homogenate was boiled for 10 min, and cell debris was pelleted by centrifugation. The supernatant was filtrated through a 0.2-μm nylon filter and analyzed using an IonPac AS9-HC column on a Dionex DX-120 ion chromatograph (http://www1.dionex.com).

To grow Arabidopsis seedlings in liquid media, 7-day-old seedlings were transferred from MS agar medium to MS liquid medium with or without NaCl and grown for 2 days with gentle agitation. For soil-grown plants, 3-week-old plants grown in soil were watered with 100 mM NaCl solution and shoots were harvested 5 days later. Samples harvested from either liquid culture or soil-grown plants were rinsed thoroughly with distilled water, dried at 75°C for 48 h, and weighed. To measure the Na^+ and K^+ content, plant samples were extracted with 1 N HNO_3 and boiled for 30 min. The Na^+ and K^+ concentrations were determined with an atomic absorption spectrophotometer (model 560; PerkinElmer, http://www.perkinelmer.com).

Yeast two-hybrid and in vitro *protein–protein interaction assay*

The *CBL10* cDNA was cloned into the activation-domain vector (pGADT7Rec) and 25 *CIPKs* were cloned into the DNA-binding domain vector (pGBT9) as described previously (Li *et al.*, 2006). AD-CBL10 and each of BD-CIPK plasmids were introduced into yeast strain PJ69-4A and selected on the synthetic complete (SC)-leucine-tryptophane agar medium. Subsequently, transformants were streaked on the SC-leucine-tryptophane-histidine agar medium supplemented with 1.5 mM 3-amino-1,2,4-aminotriazole to score growth as an indicator of the protein–protein interaction.

For expression of recombinant proteins, *CBL10* was cloned in the pET28-b(+) vector and *CIPK24* was cloned into pGEX4T-3 vector to express the proteins in *E. coli* as His-tagged form and GST fusion, respectively. Purified CBL10-His protein was mixed with GST or GST–CIPK24 fusion protein attached to glutathione-sepharose beads, as described previously (Shi *et al.*, 1999). After gentle rotation for 16 h, beads were centrifuged, washed four times with binding buffer, and eluted with 50 μl protein-loading buffer. Half the samples were resolved by sodium dodecyl sulphate–polyacrylamide-gel electrophoresis and transferred onto nitrocellulose membranes to detect CBL10-His by a Western blot procedure using anti-His antibody, as described (Shi *et al.*, 1999).

Subcellular localization and BiFC assays in planta

The cDNA of CBL10, CIPK24 or CIPK24NAFΔ was cloned into BiFC and pGPTVII-GFP5 vectors (Walter *et al.*, 2004). The CBL1, ARA6 and ARA7 constructs were as previously described (D'Angelo *et al.*, 2006; Ueda *et al.*, 2004). The TPC1 cDNA was subcloned from pART7-TPC1::GFP (Peiter *et al.*, 2005) into the binary vector pGPTVIIKan to generate an in-frame fusion with OFP. The procedure for PEG-mediated transient transformation of *Nicotiana tabacum* spp. Xanthi protoplasts was adapted from Damm *et al.* (1989) using 0.5 M mannitol and 0.1 mg l^{-1} 2,4-D, 0.2 mg l^{-1} BAP, and 1 mg l^{-1} NAA in the hormone mix. Transiently transformed protoplasts were used for co-localization of GFP::CBL10 with ARA6::mRFP. All other constructs were analyzed after infiltration of *N. benthamiana* leaves as described earlier (Walter *et al.*, 2004). Intact vacuoles from *Agrobacterium*-infiltrated *N. benthamiana* leaves were isolated according to Rentsch and Martinoia (1991). The dyes FM4-64 (Invitrogen, http://www.invitrogen.com) and 4,6-diamidino-2-phenylindole DAPI (GERBU, http://www.gerbu.de) were used at concentrations of 50 μM and 100 μg ml^{-1}, respectively. For documentation of the results, pictures were taken at room temperature with water as imaging medium and either with an inverted fluorescence microscope, Leica DMI6000B, equipped with a Leica N Plan L 20×/0,4 CORR PH1 objective, a Hamamatsu Orca camera (model C4742-80-12AG, Hamamatsu Photonics, http://www.hamamatsu.com) and guided by the OPENLAB 5.0.1 software (Improvision, http://www.improvision.com) or with an inverted microscope, Leica DMIRE2, equipped with a Leica TCS SP2 laser scanning device and the objectives HCX PL APO 63x 1,2 W Corr and HCX APO L U-V-I 63x 0,9 W using LEICA CONFOCAL ver. 2.61 software (2004). Pictures were further processed (resized and converted from tif to jpg file) using Adobe PHOTOSHOP. The background and contrast of the images were established by automatic settings in the PHOTOSHOP program.

Acknowledgments

We thank C. Eckert and S. Rips for experimental support, Dr K. Harter for enabling the ICP analyses, Dr T. Ueda for mRFP markers, Dr Yan Guo for the *sos2-2* mutant and Dr E. Peiter for providing the TPC1 construct. We are grateful to Dr E. Blumwald for helpful discussion. B.-G. Kim was supported, in part, by the National Institute of Agricultural Biotechnology, South Korea. This work was supported by grants from the DFG (AFGN Ku931/4-4) (to J.K.) and from the US Department of Agriculture and National Science Foundation (to S.L.).

Supplementary Material

The following supplementary material is available for this article online.

Figure S1. Salt sensitivity of the *cbl10* mutant can be complemented by expressing GFP::CBL10.

(a) Four-day-old Col-0, *cbl10*, *cbl4* and *sos2-2* plants were transferred to vertical 0.5 MS agar plates ± 100 mM NaCl as indicated.

(b) Four-day-old Col-0, *cbl10* and two lines of *cbl10*/pMAS:GFP::CBL10 (2 and 4) were transferred to vertical 0.5 MS agar plates ± 100 mM NaCl as indicated.

Pictures and FW measurements in (a,b) were performed 1 week after transfer. Graphs depict average values ± SE of six independent experiments.

(c) Subcellular localization of GFP::CBL10 in *cbl10*/pMAS:GFP::CBL10 plants. Left side, a leaf epidermis cell; right side, cells from the root-hair zone. Arrows indicate a membraneous invagination forming the nuclear pocket.

This material is available as part of the online article from http://www.blackwell-synergy.com

References

Albrecht, V., Weinl, S., Blazevic, D., D'Angelo, C., Batistic, O., Kolukisaoglu, U., Bock, R., Schulz, B., Harter, K. and Kudla, J. (2003) The calcium sensor CBL1 integrates plant responses to abiotic stresses. *Plant J.* **36**, 457–470.

Amtmann, A., Jelitto, T.C. and Sanders, D. (1999) K^+-selective inward-rectifying channels and apoplastic pH in barley roots. *Plant Physiol.* **120**, 331–338.

Apse, M.P. and Blumwald, E. (2002) Engineering salt tolerance in plants. *Curr. Opin. Biotechnol.* **13**, 146–150.

Apse, M.P., Aharon, G.S., Snedden, W.A. and Blumwald, E. (1999) Salt tolerance conferred by overexpression of a vacuolar Na^+/H^+ antiport in Arabidopsis. *Science*, **285**, 1256–1258.

Apse, M.P., Sottosanto, J.B. and Blumwald, E. (2003) Vacuolar cation/H^+ exchange, ion homeostasis, and leaf development are altered in a T-DNA insertional mutant of AtNHX1, the Arabidopsis vacuolar Na^+/H^+ antiporter. *Plant J.* **36**, 229–239.

Arnon, D.J. (1949) Copper enzymes in isolated chloroplasts. Polyphenoloxidase in *Bela vulgaris*. *Plant Physiol.* **24**, 1–15.

Barnes, J.D., Balaguer, L., Manrique, E., Elvira, S. and Davison, A.W. (1992) A reappraisal of the use of DMSO for the extraction and determination of chlorophylls *a* and *b* in lichens and higher plants. *Env.* Exp. Bot. **32**, 85–100.

Batistic, O. and Kudla, J. (2004) Integration and channeling of calcium signaling through the CBL calcium sensor/CIPK protein kinase network. *Planta*, **219**, 915–924.

Berthomieu, P., Conejero, G., Nublat, A. *et al.* (2003) Functional analysis of AtHKT1 in Arabidopsis shows that $Na^{(+)}$ recirculation by the phloem is crucial for salt tolerance. *EMBO J.* **22**, 2004–2014.

Blumwald, E. (2000) Sodium transport and salt tolerance in plants. *Curr. Opin. Cell Biol.* **12**, 431–434.

Cheong, Y.H., Kim, K.N., Pandey, G.K., Gupta, R., Grant, J.J. and Luan, S. (2003) CBL1, a calcium sensor that differentially regulates

salt, drought, and cold responses in Arabidopsis. *Plant Cell*, **15**, 1833–1845.

Clough, S.J. and Bent, A.F. (1998) Floral dip: a simplified method for *Agrobacterium*-mediated transformation of *Arabidopsis thaliana*. *Plant J.* **16**, 735–743.

D'Angelo, C., Weinl, S., Batistic, O. *et al.* (2006) Alternative complex formation of the Ca^{2+}-regulated protein kinase CIPK1 controls abscisic acid-dependent and independent stress responses in Arabidopsis. *Plant J.* **48**, 857–872.

Damm, B., Schmidt, R. and Willmitzer, L. (1989) Efficient transformation of *Arabidopsis thaliana* using direct gene transfer to protoplasts. *Mol. Gen. Genet.* **217**, 6–12.

Dettmer, J., Hong-Hermesdorf, A., Stierhof, Y.-D. and Schumacher, K. (2006) Vacuolar H^+-ATPase activity is required for endocytic and secretory trafficking in Arabidopsis. *Plant Cell*, **18**, 715–730.

Flowers, T.J., Koyama, M.L., Flowers, S.A., Sudhakar, C., Singh, K.P. and Yeo, A.R. (2000) QTL: their place in engineering tolerance of rice to salinity. *J. Exp. Bot.* **51**, 99–106.

Hasegawa, P.M., Bressan, R.A., Zhu, J.K. and Bohnert, H.J. (2000) Plant cellular and molecular responses to high salinity. *Annu. Rev. Plant Physiol. Plant Mol. Biol.* **51**, 463–499.

Hedrich, R. and Kudla, J. (2006) Calcium signaling networks channel plant K^+ uptake. *Cell*, **125**, 1221–1223.

Hu, C.-D. and Kerppola, T. K. (2003) Simultaneous visualization of multiple protein interactions in living cells using multicolor fluorescence complementation analysis. *Nature Biotech.* **21**, 539–545.

Knight, H. (2000) Calcium signaling during abiotic stress in plants. *Int. Rev. Cytol.* **195**, 269–324.

Kolukisaoglu, U., Weinl, S., Blazevic, D., Batistic, O. and Kulda, J. (2004) Calcium sensors and their interacting protein kinases: genomics of the Arabidopsis and rice. *Plant Physiol.* **134**, 43–58.

Lee, G.J., Sohn, E.J., Lee, M.H. and Hwang, I. (2004) The Arabidopsis rab5 homologs rha1 and ara7 localize to the prevacuolar compartment. *Plant Cell Physiol.* **45**, 1211–1220.

Li, L., Kim, B.G., Cheong, Y.H., Pandey, G.K. and Luan, S. (2006) A $Ca^{(2)+}$ signaling pathway regulates a $K^{(+)}$ channel for low-K response in Arabidopsis. *Proc. Natl Acad. Sci. USA*, **103**, 12625–12630.

Liu, J. and Zhu, J.K. (1998) A calcium sensor homolog required for plant salt tolerance. *Science*, **280**, 1943–1945.

Luan, S., Kudla, J., Rodriguez-Concepcion, M., Yalovsky, S. and Gruissem, W. (2002) Calmodulins and calcineurin B-like proteins: calcium sensors for specific signal response coupling in plants. *Plant Cell*, **14**, S389–S400.

Munns, R., James, R.A. and Lauchli, A. (2006) Approaches to increasing the salt tolerance of wheat and other cereals. *J. Exp. Bot.* **57**, 1025–1043.

Niu, X., Narasimhan, M.L., Salzman, R.A., Bressan, R.A. and Hasegawa, P.M. (1993) NaCl regulation of plasma membrane $H^{(+)}$-ATPase gene expression in a glycophyte and a halophyte. *Plant Physiol.* **103**, 713–718.

Pandey, G.K., Cheong, Y.H., Kim, K.N., Grant, J.J., Li, L., Hung, W., D'Angelo, C., Weinl, S., Kudla, J. and Luan, S. (2004) The calcium sensor calcineurin B-like 9 modulates abscisic acid sensitivity and biosynthesis in Arabidopsis. *Plant Cell*, **16**, 1912–1924.

Pardo, J.M., Cubero, B., Leidi, E.O. and Quintero, F.J. (2006) Alkali cation exchangers: roles in cellular homeostasis and stress tolerance. *J. Exp. Bot.* **57**, 1181–1199.

Peiter, E., Maathuis, F.J.M., Mills, L.N., Knight, H., Pelloux, J., Hetherington, A.M. and Sanders, D. (2005) The vacuolar Ca^{2+}-activated channel TPC1 regulates germination and stomatal movement. *Nature*, **434**, 404–408.

Qiu, Q.S., Barkla, B.J., Vera-Estrella, R., Zhu, J.K. and Schumaker, K.S. (2003) Na^+/H^+ exchange activity in the plasma membrane of Arabidopsis. *Plant Physiol.* **132**, 1041–1052.

Qiu, Q.S., Guo, Y., Quintero, F.J., Pardo, J.M., Schumaker, K.S. and Zhu, J.K. (2004) Regulation of vacuolar Na^+/H^+ exchange in *Arabidopsis thaliana* by the salt-overly-sensitive (SOS) pathway. *J. Biol. Chem.* **279**, 207–215.

Ren, Z.H., Gao, J.P., Li, L.G., Cai, X.L., Huang, W., Chao, D.Y., Zhu, M.Z., Wang, Z.Y., Luan, S. and Lin, H.X. (2005) A rice quantitative trait locus for salt tolerance encodes a sodium transporter. *Nature Genet.* **37**, 1141–1146.

Rentsch, D. and Martinoia, E. (1991) Citrate transport into barley mesophyll vacuoles – comparison with malate uptake activity. *Planta*, **184**, 532–537.

Rus, A., Lee, B.H., Munoz-Mayor, A., Sharkhuu, A., Miura, K., Zhu, J.K., Bressan, R.A. and Hasegawa, P.M. (2004) AtHKT1 facilitates Na^+ homeostasis and K^+ nutrition *in planta*. *Plant Physiol.* **136**, 2500–2511.

Sanders, D., Pelloux, J., Brownlee, C. and Harper, J.F. (2002) Calcium at the crossroads of signaling. *Plant Cell*, **14**, S401–S417.

Shi, J., Kim, K.N., Ritz, O., Albrecht, V., Gupta, R., Harter, K., Luan, S. and Kudla, J. (1999) Novel protein kinases associated with calcineurin B-like calcium sensors in Arabidopsis. *Plant Cell*, **11**, 2393–2405.

Shi, H., Quintero, F.J., Pardo, J.M. and Zhu, J.K. (2002) The putative plasma membrane $Na^{(+)}/H^{(+)}$ antiporter SOS1 controls long-distance $Na^{(+)}$ transport in plants. *Plant Cell*, **14**, 465–477.

Ueda, T., Yamaguchi, M., Uchimiya, H. and Nakano, A. (2001) ARA6, a plant-unique novel type Rab GTPase, functions in the endocytic pathway of *Arabidopsis thaliana*. *EMBO J.* **20**, 4730–4741.

Ueda, T., Uemura, T., Sato, M.H. and Nakano, A. (2004) Functional differentiation of endosomes in Arabidopsis cells. *Plant J.* **40**, 783–789.

Walter, M., Chaban, C., Schütze, K. *et al.* (2004) Visualization of protein interactions in living plant cells using bimolecular fluorescence complementation. *Plant J.* **40**, 428–438.

White, P.J., Bowen, H.C., Demidchik, V., Nichols, C. and Davies, J.M. (2002) Genes for calcium-permeable channels in the plasma membrane of plant root cells. *Biochim. Biophys. Acta*, **1564**, 299–309.

Wu, S.J., Ding, L. and Zhu, J.K. (1996) *SOS1*, a genetic locus essential for salt tolerance and potassium acquisition. *Plant Cell*, **8**, 617–627.

Xu, J., Li, H.D., Chen, L.Q., Wang, Y., Liu, L.L., He, L. and Wu, W.H. (2006) A protein kinase, interacting with two calcineurin B-like proteins, regulates K^+ transporter AKT1 in Arabidopsis. *Cell*, **125**, 1347–1360.

Yeo, H., Kim, K.W., Kim, J. and Choi, Y.H. (1998) Steroidal glycosides of the 14,15-seco-18-nor-pregnane series from *Cynanchum ascyrifolium*. *Phytochemistry*, **49**, 1129–1133.

Yokoi, S., Quintero, F.J., Cubero, B., Ruiz, M.T., Bressan, R.A., Hasegawa, P.M. and Pardo, J.M. (2002) Differential expression and function of *Arabidopsis thaliana* NHX Na^+/H^+ antiporters in the salt stress response. *Plant J.* **30**, 529–539.

Zhu, J.K. (2003) Regulation of ion homeostasis under salt stress. *Curr. Opin. Plant Biol.* **6**, 441–445.

